



## Development of a 3D CZT detector prototype for Laue Lens telescope

**Caroli, Ezio; Auricchio, Natalia; Del Sordo, Stefano; Abbene, Leonardo; Budtz-Jørgensen, Carl; Casini, Fabio; Curado da Silva, Rui M.; Kuvvetli, Irfan; Milano, Luciano; Natalucci, Lorenzo**

*Total number of authors:*  
15

*Published in:*  
Proceedings of SPIE - The International Society for Optical Engineering

*Link to article, DOI:*  
[10.1117/12.858120](https://doi.org/10.1117/12.858120)

*Publication date:*  
2010

*Document Version*  
Publisher's PDF, also known as Version of record

[Link back to DTU Orbit](#)

*Citation (APA):*  
Caroli, E., Auricchio, N., Del Sordo, S., Abbene, L., Budtz-Jørgensen, C., Casini, F., Curado da Silva, R. M., Kuvvetli, I., Milano, L., Natalucci, L., Quadrini, E. M., Stephen, J. B., Ubertini, P., Zanichelli, M., & Zappettini, A. (2010). Development of a 3D CZT detector prototype for Laue Lens telescope. *Proceedings of SPIE - The International Society for Optical Engineering*, 7742, 77420V. <https://doi.org/10.1117/12.858120>

---

### General rights

Copyright and moral rights for the publications made accessible in the public portal are retained by the authors and/or other copyright owners and it is a condition of accessing publications that users recognise and abide by the legal requirements associated with these rights.

- Users may download and print one copy of any publication from the public portal for the purpose of private study or research.
- You may not further distribute the material or use it for any profit-making activity or commercial gain
- You may freely distribute the URL identifying the publication in the public portal

If you believe that this document breaches copyright please contact us providing details, and we will remove access to the work immediately and investigate your claim.

# Development of a 3D CZT detector prototype for Laue Lens telescope

Ezio Caroli<sup>1a</sup>, Natalia Auricchio<sup>a</sup>, Stefano del Sordo<sup>b</sup>, Leonardo Abbene<sup>b</sup>, Carl Budtz-Jørgensen<sup>c</sup>,  
Fabio Casini<sup>d,i</sup>, Rui M. Curado da Silva<sup>e</sup>, Irfan Kuvvetli<sup>c</sup>, Luciano Milano<sup>f</sup>, Lorenzo Natalucci<sup>g</sup>,  
Egidio M. Quadrini<sup>d</sup>, John B. Stephen<sup>a</sup>, Pietro Ubertini<sup>g</sup>,  
Massimiliano Zanichelli<sup>h</sup>, Andrea Zappettini<sup>h</sup>.  
<sup>a</sup>INAF/IASF-Bologna, Via Gobetti 101; 40129 Bologna, Italy  
<sup>b</sup>INAF/IASF-Palermo, Via Ugo La Malfa 153, 90146 Palermo, Italy  
<sup>c</sup>National Space Institute/DTU, Juliane Maries Vej 30, DK 2100 Copenhagen, Denmark  
<sup>d</sup>INAF/IASF-Milano, Via E. Bassini 15, 20133 Milano (Italy)  
<sup>e</sup>Universidade de Coimbra, Departamento de Física, Rue Larga P-3004 516 Coimbra, Portugal  
<sup>f</sup>Dipartimento di Fisica, Università di Ferrara, Via Saragat 1, 44100 Ferrara, Italy  
<sup>g</sup>INAF/IASF-Roma, Via Fosso del Cavaliere 100, 0133 Roma, Italy  
<sup>h</sup>CNR/IMEM, Parco Area delle Scienze 37/A - 43100 Parma, Italy  
<sup>i</sup>Sanitas EG srl, 20133 Milano, Italy

## ABSTRACT

We report on the development of a 3D position sensitive prototype suitable as focal plane detector for Laue lens telescope. The basic sensitive unit is a drift strip detector based on a CZT crystal, ( $\sim 19 \times 8$  mm<sup>2</sup> area, 2.4 mm thick), irradiated transversally to the electric field direction. The anode side is segmented in 64 strips, that divide the crystal in 8 independent sensor (pixel), each composed by one collecting strip and 7 (one in common) adjacent drift strips. The drift strips are biased by a voltage divider, whereas the anode strips are held at ground. Furthermore, the cathode is divided in 4 horizontal strips for the reconstruction of the third interaction position coordinate. The 3D prototype will be made by packing 8 linear modules, each composed by one basic sensitive unit, bonded on a ceramic layer. The linear modules readout is provided by a custom front end electronics implementing a set of three RENA-3 for a total of 128 channels. The front-end electronics and the operating logics (in particular coincidence logics for polarisation measurements) are handled by a versatile and modular multi-parametric back end electronics developed using FPGA technology.

**Keywords:** CZT detector, gamma ray spectroscopy, drift strip, 3D imaging, hard X- and soft gamma-ray astronomy

## 1. INTRODUCTION

The large number of results obtained with the most recent satellite missions on many classes of high energy celestial sources have demonstrated the importance of a broad band spectroscopy extending up several hundreds of keV. Recently both ESA<sup>1</sup> and NASA have indicated in their guidelines for the progress of X- and  $\gamma$ -ray astronomy in the next decade the development of new instrumentation working in the energy range from the keV to the MeV region, where many important scientific issues are still open. In this perspective the development of new instrumentation based on concentrating (e.g. multilayer mirror) telescopes for hard X-rays (1-100 keV) and focusing instruments based on broad band Laue lenses operating from about 60 keV up to the MeV region is particularly challenging<sup>2</sup>.

To exploit the performance of both multilayer Hard X ray mirrors and Laue lenses, focal plane detectors with high efficiency (80% up to 1 MeV) and fine spectroscopy (e.g. a few % FWHM at 100 keV) and with a moderate spatial resolution (between 0.5 and 2 mm) are required. Furthermore, the use of focal plane detectors for such applications which are sensitive to the photon interaction position in three dimensions will allow the implementation of more efficient background rejection techniques. Finally, we point out that the high spatial segmentation of the needed focal plane detectors and the required spectroscopic performance will allow to use this new instrumentation to perform very

<sup>1</sup> [caroli@iasfbo.inaf.it](mailto:caroli@iasfbo.inaf.it), phone: +390516398678, fax: +390516398723

sensitive measurements of the flux polarization level from high energy sources<sup>3</sup>, that is today one of the hot topics in high energy astronomy.

As demonstrated by several groups working on this technology, one of the most promising materials for the construction of position sensitive spectrometers with the required characteristics is Cadmium Zinc Telluride (CZT). CZT detectors have been the subject of great attention from the scientific community interested in applications in X- and  $\gamma$ -rays, particularly for the realisation of spectroscopic imagers for exploration of the universe<sup>4,5,6</sup>. The present work is inserted in this international contest being oriented to the development of an innovative concept of 3D position sensitive spectrometers that could be very suitable for application focal plane for a Laue lens telescope for future hard X and soft gamma ray mission. Laue lens telescope operating up to the MeV region require very efficient focal plane to avoid significant loss of the focussed photons that would reduced sensitivity of the instrument and then would waste the advantages of focusing. This high detection efficiency, that shall be achieved maintaining fine spectroscopy and good spatial resolution, can be obtained only using high Z materials and stack of several<sup>7,8</sup>.

Herein we describe the development of a demonstrative prototype of a wide band Laue lens 3D focal plane detector<sup>9</sup>. Despite its reduced size (4 cm<sup>2</sup>, 128 active channels, 8 mm thickness) the proposed prototype will implement several significant features to obtain high efficiency with improved spectroscopy coupled with three dimensional spatial resolution of few mm. The detector design is based on an array of CZT sensors. Each sensitive unit implements a particular irradiation configuration with a drift micro-strip anode that allows to achieve a good, and independent from photon interaction positions, spectroscopic response. The further segmentation on the cathode side of each CZT unit allows to obtain the third spatial coordinate and to work with a single detector layer in a manner equivalent to a stack, but with no passive material between each layer. In the following sections we describe the current status of the prototype construction starting from the configuration of the basic CZT sensitive unit, through the assembling of the spectrometer linear module, to the final 3D position sensitive spectrometer prototype as well as the development of the dedicated analogue front-end electronics and data handling system.

## 2. THE BASIC CZT SENSITIVE UNIT

The 3D prototype is based on the use of CZT crystals in the Planar Transverse Field (PTF) configuration, as proposed by our group in the 1990's<sup>10</sup>, in which the direction of the incoming photons (i.e. the optical axis of the sensor) is perpendicular to the to the electrical field lines direction. This configuration allows to increase the photon absorption thickness up to few centimeters without increasing the charge collection distance (i.e. avoiding severe spectroscopic performance degradation). The drawback of the PTF irradiating geometry is that all the positions between the collecting electrodes are uniformly hit by radiation leading to a stronger effect of the difference in charge collection efficiency in the spectroscopic performance with respect to the standard Parallel Planar Field (PPF) irradiation configuration through the cathode.

Therefore in order to recover from this spectroscopic degradation and to improve the CZT sensitive unit performance, we have decided to use an anode made of an array of micro-strips in a drift configuration: a thin collecting anode strip surrounded by guard strips with decreasing bias voltage. This anode configuration, proposed and studied at NSI/DTU in Copenhagen<sup>11,12</sup>, allows the detector to become almost a single charge carrier device (i.e. the signal depend only on the electron collection), avoiding the degradation of the spectroscopic response by the charge loss due to the hole trapping and providing a more uniform spectroscopic response (i.e. independent from the distance of the interaction from the collecting electrodes as shown in Figure 2. In addition, it will possible to perform a further compensation of the collected charge signals using the photon interaction position that can be inferred by the ratio between the cathode and the anode strip signals.

Finally in order to obtain 3D sensitivity for the photon interaction position, the cathode is segmented into 4 strips in the direction orthogonal to the anode ones. Therefore the final prototype becomes equivalent to a stack of thinner CZT horizontal layers with the advantage of not having any passive material between each layer.

### 2.1 The adopted CZT sensitive unit configuration

The final CZT sensor units (Figure 1) were realized by Quik-Pak (CA, USA) cutting 8 single crystals of 19.35×8×2.4 mm<sup>3</sup> from REDLEN Tech. (BC, Canada) CZT wafers. On the anode side, the microstrip set is divided in 8 equivalent pixels with a pitch of 2.4 mm, being only 8 strips connected to the readout electronics, while the others act as drift strips used to shape the charge collecting field, through a proper decreasing bias scheme explained in section 3. Each collecting

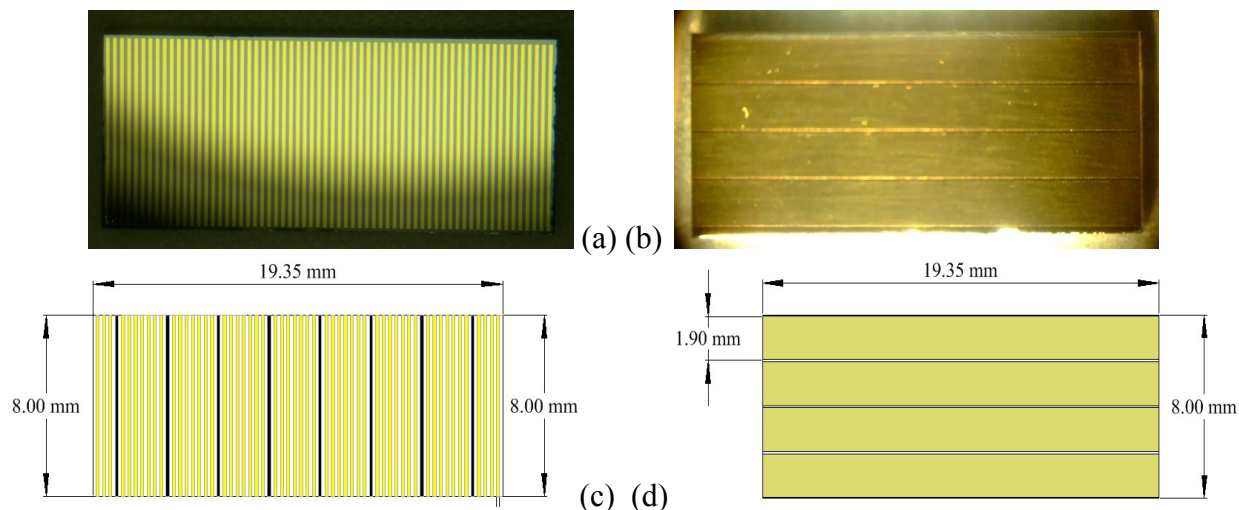


Figure 1. The CZT sensitive unit seen from the anode (a) and the cathode (b) side. The schematic drawing of the CZT sensitive unit of two collecting crystal sides is shown in (c-d). In particular (c) highlight the 8 proper anode strips (dark) from the drift ones (light).

strip is surrounded by 4 drift strips on each side, with the central one shared. In total, the anode side is composed by 64 metallic (Ni/Au)  $\mu$ -strips 0.15 mm wide with a gap of the same size. The cathode side is made by a set of 4 metallic strips that are orthogonal to the anode ones with a pitch of 2 mm (1.9 mm wide Ni/Au metallisation with a 0.1 mm gap).

## 2.2 Expected CZT unit spectroscopic performance

In order to assess the expected spectroscopic performance of the working configuration of our CZT units and therefore of the final 3D prototype, we have performed several tests in the PTF irradiating configuration using a CZT drift strip detector available at the DTU in Copenhagen. This sensor, built by eV Products (PA, USA) on a  $10 \times 10 \times 2.5$  mm<sup>3</sup> CZT crystal, is very similar in dimensions and in electrode configuration with our detector units, being the anode side composed by a set of Pt/Au strips with 0.1 mm width and a pitch of 0.2 mm. As in our CZT sensors, each anode strip is surrounded on each side by 4 drift strips. The anode readout strips are held at ground potential, while the drift strips are negatively biased using a voltage divider providing  $V_i = -i \cdot V_d / 4$ , where  $V_d$  is main drift strip bias voltage. On the opposite side, the cathode is realized by a single Pt metallic layer, that is negatively biased. The readout strips and the cathode were connected to eV-550 preamplifiers, main shaping amplifiers and then to a multi-parameter data acquisition system. For these measurements <sup>57</sup>Co, <sup>109</sup>Cd and <sup>137</sup>Cs radioactive sources were used in both PTF and PPF configurations to compare the results and to verify the prediction. The measurements have been performed using 1  $\mu$ s shaping time,  $V_p = -150$  V as cathode bias, and  $V_1 = -30$  V,  $V_2 = -60$  V,  $V_3 = -90$  V,  $V_4 = -120$  V as drift strip bias voltage.

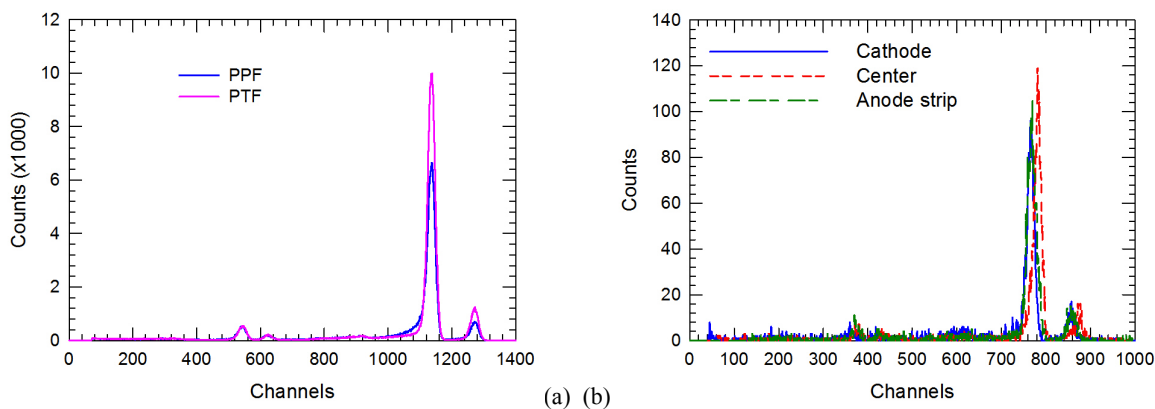


Figure 2. (a) The uncollimated <sup>57</sup>Co spectrum obtained in PTF and PPF irradiating configuration using the DTU CZT sensor; (b) collimated PTF spectra at three different positions between the collecting electrodes.



Figure 2(a) compares the spectra obtained by irradiating all the region centred on anode strip 3 in both PPF and PTF configuration with a  $^{57}\text{Co}$  source placed inside 11 cm length Pb collimator with a 0.6 mm  $\varnothing$  hole and positioned at 13 cm from the CZT exposed area. The energy resolutions for the two spectra are equal, being slightly better 3% (FWHM) in both cases, but the PTF configuration provides as expected a better efficiency compared to PPF with increasing energy. In fact, the almost perfect Gaussian shape of the full energy peaks in the spectra clearly demonstrates the good charge collection properties guaranteed by the drift strips configuration implemented on the CZT anode side. The effectiveness of a drift strips anode in improving the spectroscopic performance of a CZT sensor is further confirmed by the spectra shown in the Figure 2(b). These spectra were obtained by irradiating the CZT detector in PTF configuration with the source beam finely collimated (0.2 mm hole) at three different position between the collecting electrodes. The results demonstrate the almost complete independence of the spectroscopic response from the position of the photon interaction with respect to the collecting electrodes as the full energy peak channel do not significantly change ( $\sim 2\%$ ) and the energy resolution slightly increases as expected moving toward the anode<sup>13</sup>.

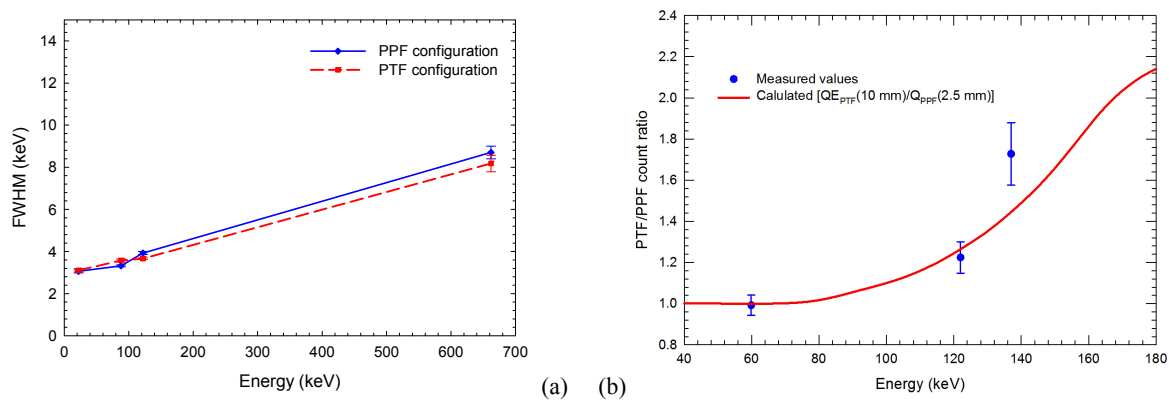


Figure 3. (a) The energy resolution measured using the DTU CZT drift strip sensor both in PTF and PPF irradiation configuration; (b) The ratio between counts integrated under the full energy peaks obtained in PTF and PPF configurations (dot) compared with the expected quantum efficiency ratio (solid line).

Figure 3 summarizes the results of the tests in energy resolution and detection efficiency obtained with the DTU detector in both PPF and PTF configuration. As shown in the (a) graph, the measured energy resolutions for PTF and PPF configuration are equal, within errors, over the entire explored energy range. The PTF configuration provides a slightly better energy resolution at the highest energy (662 keV). In order to evaluate the detection efficiency gain in the PTF irradiation configuration with respect to the PPF one, we have calculated the ratio between the full energy peaks integrated counts in the two cases using the measured  $^{57}\text{Co}$  spectra (57.5 keV from the Ta source shield, 122 keV, 136 keV). These values are reported in Figure 3 (b) superimposed to the theoretical ratio of quantum efficiencies (QE) for a 10 mm thick CZT used in PTF and a 2.5 mm thick used in PPF irradiation configuration. The measured PTF/PPF ratio values are in good agreement with the expected theoretical  $\text{QE}_{\text{PTF}}(10 \text{ mm})/\text{QE}_{\text{PPF}}(2.5 \text{ mm})$  values for CZT material, demonstrating the expected detection efficiency improvement of the PTF configuration above  $\sim 80$  keV.

### 3. THE 3D POSITION SENSITIVE SPECTROMETER PROTOTYPE

The construction of the final 3D position sensitive spectrometer prototype foresees a the first step the realization of a set of drift strip CZT sensor linear modules. To build these modules we use a thin ceramic layer ( $\text{Al}_2\text{O}_3$ ) on which each CZT sensor will be glued in a cavity at the centre of the alumina layer in order to have its anode side coplanar with one side of the supporting layer as shown in Figure 4 (a). We have made this choice in order to facilitate bonding procedure with the fine pitch  $\mu$ -strips pattern on the CZT anode side. The bonding between the CZT anode side strips and the metallic pads on the alumina layer will be realized using thin (50  $\mu\text{m}$ ) Cu comb obtained by photo engraving technique having the same pattern of the anode side strips with low temperature soldering paste. On this side of the support only the metallic traces to bias the drift strips and to readout the 8 anode signals are implemented providing the connection to coupling and filter circuitry and finally to I/O linear module pins by metalized vias. In fact all the passive components needed to realize both the voltage divider for drift strips bias, the cathode HV bias and the coupling of strips signals (anode and cathode) to the analogue readout electronics are mounted on the opposite side in order to use the space leaved free by the net thickness of the detector (1.8 mm).

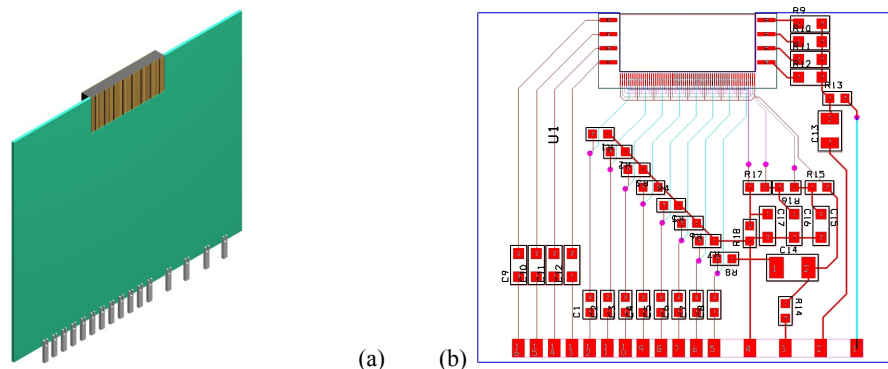


Figure 4. (a) The 3D schematic view of the linear module showing the mounting of the CZT sensor; (b) The linear module support electrical layout showing the I/O pads (bottom), the voltage divider circuitry to provide the drift strip operating bias (centre) and the CZT sensor bonding pads (top).

The electrical layout of the linear module is shown in Figure 4(b) seen from the cathode side. The four I/O pad on the right are dedicated to the bias circuitry, while the 12 ones at left are dedicated to readout the cathode (4) and anode (8) signals. In particular it is visible on the right the voltage divider to set the operating bias to each drift strip starting from a single independent voltage provided by a dedicated DC-DC converter on the analogue front-end electronics board. On the top right there are the capacitor and the resistors for cathode strips HV bias, while above the signal readout pins are visible the SMD components needed to couple the signals to the ASIC's input channels in the front-end electronics. The line in light colours are in fact on the opposite side of the alumina layer, the small circles representing the vias used to electrically connect the traces implemented on the two sides. The complete 8 CZT linear modules are under realization by Aurel S.p.A (Modigliana, Italy) using standard 0.6 mm thick alumina layers of  $60 \times 50 \text{ mm}^2$ .

### 3.1 The 3D position sensitive spectrometer prototype box

The final step to build the 3D position sensitive prototype is the packaging of the 8 linear modules in order to obtain the  $8 \times 8 \times 4$  voxels (cubic pixels) detector. The packaging of the linear modules will be guarantee by a custom Al box designed to provide both the linear module mechanical support minimizing the gap between each module (3.5 mm) and the interface with the analogue front-end electronics (AFEE) board. The drawing of the detector box is shown in Figure 5. The mechanical support foresees the possibility to temperature and humidity control by fluxing dry air or Nitrogen through two valves that are visible on the bottom flange and guarantee both a good electromagnetic shield and light tight environment for the entire detector. The photon entrance window on the box top cover will be realized using a 0.1 mm thick Be layer of  $25 \times 45 \text{ mm}^2$  in order to reduce the photon absorption at low energies ( $< 10 \text{ keV}$ ). Each CZT linear module is keep in position through Teflon guides that grab the  $\text{Al}_2\text{O}_3$  layer at the empty space (10 mm) leaved on each vertical side. This solution will allow an easy insertion and extraction of each linear module in and from the electrical connectors aligned below the detector on the analogue front end electronics board. The detector box is directly bolted to the AFEE board trough a metallic contact that provides a separate ground.

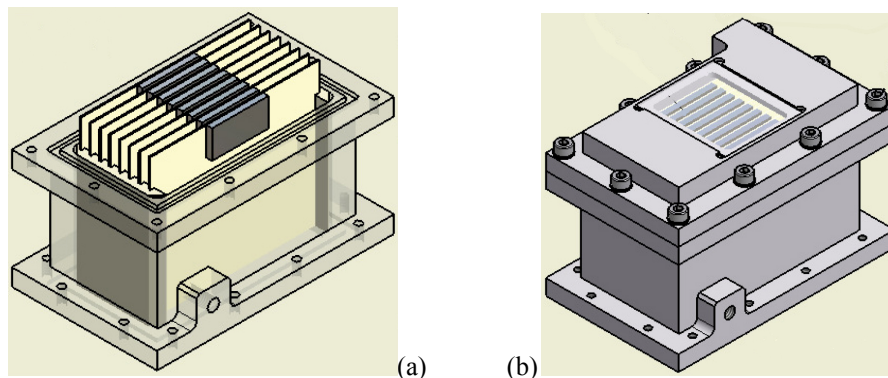


Figure 5. The 3D position sensitive spectrometer prototype packaging (a) and the overall view of the detector box (b) with the Be window and N/Dry air flux pipe on the bottom flange.

#### 4. THE ANALOG FRONT-END ELECTRONICS

The main function of the analogue front-end electronics (AFEE) is to connect the 64 anode strips and the 32 cathodes to three RENA-3 ASIC from NOVA R&D Inc. (CA, USA) used as signal readout devices. The RENA-3 ASIC is a 36-channel charge sensitive amplifier self-triggering. Each channel includes a low-noise preamplifier, a shaper with sample/hold, and in addition a fast shaper that gives a trigger signal for coincident event detection. The signal range is selectable channel by channel over two full scales (equivalent to 200 keV and 1.3 MeV for CZT) as the peaking time that ranges from 0.1 to 40  $\mu$ s. The comparator thresholds can be adjusted through an 8 bit DAC on each channel in order to obtain an accurate and uniform threshold setting. A pole-zero cancellation circuit is available for minimizing pileup errors. All these features are selectable by software and are independent for each input channel.

Preliminary measurements were performed using a demo board, illustrated in Figure 6, developed to test the chip functionalities before the final implementation on the AFEE. This demo board is composed of two parts: the CPU board on the left and the RENA-3 board on the right. The CPU manages the ASIC configuration and receives the output data using a custom acquisition software. The RENA-3 board provides the low bias voltages (DAC reference voltages and power supplies), calibration pulser and CPU interface. Furthermore the monitors of the pulser signal and the RENA-3 analog output are available. The dynamic range was determined by charge injection using a voltage step at the test input, which feeds a  $\sim 75$  fF internal capacitor that can be switched to any input channel. Figure 7(a) reports the output amplitude measured for the minimum and maximum gain as a function of the injecting charge. The measured dynamic range for gain 1.6 is linear up to 36 fC and the chip output saturates at  $\sim 40$  fC (1.15 MeV), for gain 5 the dynamic range is linear up to 9 fC and the chip output saturates at  $\sim 15$  fC (435 keV). The distribution of the noise and offset values is shown in Figure 7(b-c): the gaussian fit gives a noise of  $(8.95 \pm 0.50)$  keV and an offset mean value of  $(-673.62 \pm 11.86)$  mV.

In the AFEE several other functions are implemented such as the detector high voltage power supply, the low voltage power supply, the conditioning electronics, the low and high voltage monitors, two temperature and humidity sensors for monitoring the detector and electronics environmental operating conditions.

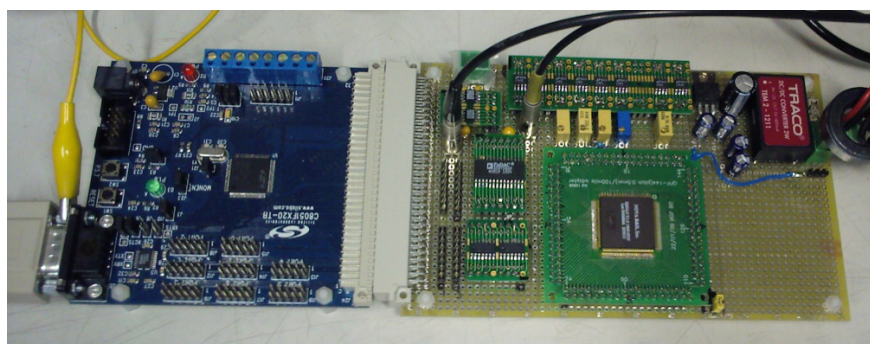


Figure 6. The test board developed (right) to evaluate the RENA-3 chip performance and to tune the AFEE board design connected to the FPGA units used control and acquire the ASIC.

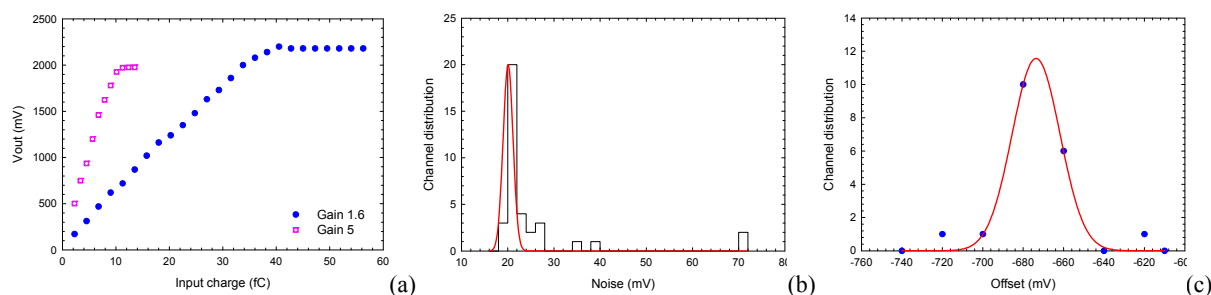


Figure 7. Measurement of the dynamic range for the two different ASIC gains (a). Measurement of the electronic noise (b) and the offset values (c).

## 4.1 The AFEE final design

The view of the final AFEE board layout is shown in Figure 8. The AFEE is currently under construction using a 6 layers FR4 board. On the top side the detector box interface with eight linear module connectors is visible at the board centre. The three RENA-3 ASICs are mounted on the AFEE bottom side distributed around the detector footprint. In order to reduce the parasitic capacitances care has been taken in minimizing the trace length from the detector output pins to the chip input channels. Two independent low ripple DC-DC converters are located on the board (the two dark boxes) at one side providing both the cathode and the anode drift strips polarization voltages. Between these two units the circuits for low bias voltages generation and monitoring of the AFEE and daughter board (see the next section) are implemented. The analog and digital RENA-3 power supplies as well as the reference voltages to manage the analog output signals are located on board top side in correspondence with the three chips position on the bottom side. The RENA-3 analog output signals are buffered and sent to daughter card ADCs. An additional feature of the AFEE board is the capability of calibrating each ASIC channel using an on board pulser. The horizontal box highlight the I/O high density connectors to the data handling electronics. The maximum expected AFEE power consumption is 26 W.

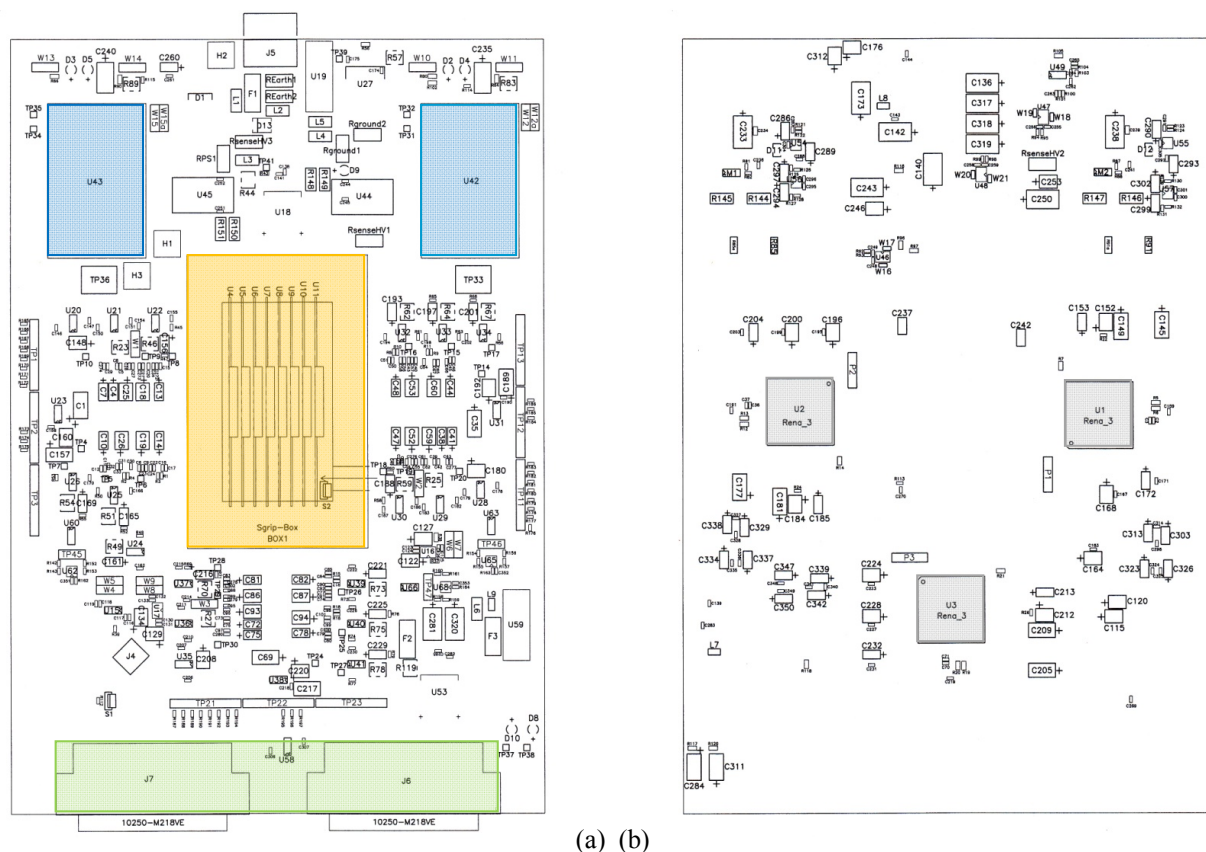


Figure 8. The final layout of the AFEE board: (a) top view from the detector box; (b) bottom view.

## 5. THE DATA HANDLING ELECTRONICS SYSTEM

The Data Handling Electronics (DHE) is composed of a daughter board (SG\_ADC) that provides the interface between the AFEE and main digital processing board (SG\_DGT). Its functional scheme is shown in Figure 9. The DHE manages the detector high voltage power supply, the analog signal offset level A/D converters, the ASIC parameters configuration, the coincidence logics, the detector operational parameters, and finally prepares the output data stream using a programmable data format (LABVIEW compatible). The DHE system is based on a FPGA with embedded Power PC (PPC) and will be able to handle up to 128 independent channels via an Ethernet link.



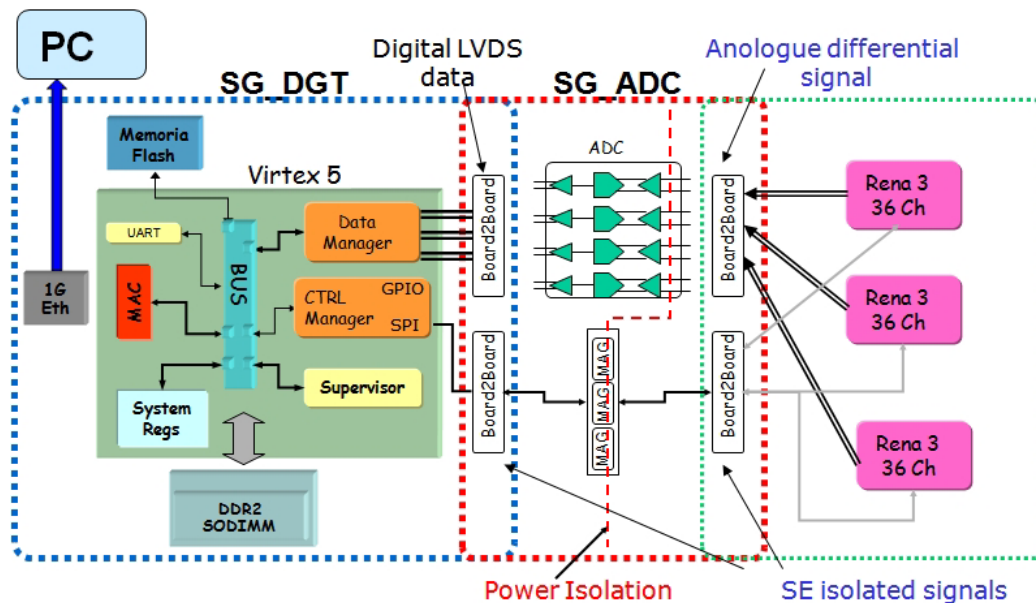


Figure 9. The functional and configuration scheme of the Data Handling Electronics (DHE) system. The two box highlighted by thick border are the two DHE subsystems, while the one at right represent the AFEE board.

### 5.1 The daughter board

The daughter board is placed on top of the SG\_DGT one in the same metallic container and provides the interface circuits between the SG\_DGT and the AFEE board, as well as the DAC and the ADC conversions. The main interface circuits consist of galvanic isolators for the digital signals from the SG\_DGT to the AFEE board. One fast DAC is used to calibrate each RENA-3 channel, while others DACs set the high voltage values and the ADC read the high voltage analog monitors. Finally the daughter board provides the A/D conversion of the RENA-3 analog signals.

### 5.2 The digital processing board

The digital processing board (Figure 10) implement a Xilinx Virtex5 FPGA with embedded PPC and up to 2GB of local memory to manage the chip functionalities through an 1G Ethernet connection. Each acquisition module, composed of the RENA-3 ASIC and relative ADC, is managed by an IP-core that allows to adjust the ASIC settings, processes the received data and sends it to remote PC via Ethernet performing the data formatting. In particular the SG\_DGT can operate in coincidence mode acquiring events with any multiplicity in a selectable window from 1 to 20  $\mu$ s. The full operating configuration can be store in the flash memory and reloaded automatically at every system startup. The digital processing board has been designed to manage up to 50k events/sec.

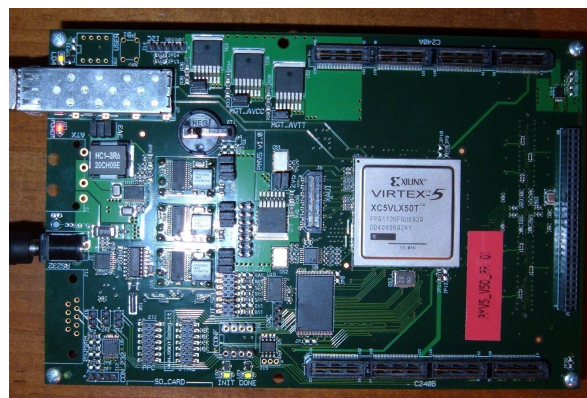


Figure 10. The digital processing board (SG\_DGT). At the right it is visible the connector to the daughter board.

## 6. CURRENT DEVELOPMENT STATUS AND CONCLUSIONS

Currently almost all the prototype subsystems and mechanics are under construction and their delivery is foreseen within a working month. Only concerning the linear module realisation there are still some preliminary activities undergoing to verify the validity of the chosen bonding technique with some dummy CZT sensors realized by the IMEM/CNR group<sup>14</sup>.

We foresee the integration and functional tests of AFEE and DHE in the next September, while we expect to have all the CZT linear modules ready to be implemented in the prototype a month later. The laboratory performance tests using radioactive sources, of the 3D CZT prototype could therefore start within the end of this year. Meanwhile we intend to submit a proposal to ESRF in Grenoble (France) to perform measurements with a high energy (50-700 keV) polarised photon beam at the line ID15A. The features of this beam line will allow us to characterise, over a wide energy range, with different beam size and as function of the photon incidence angles, our prototype in imaging capabilities, spectroscopic performance and effectiveness as scattering polarimeter<sup>15</sup>.

An important activity, that is held in parallel with the construction of the prototype, is the implementation in GEANT 4 of a numerical model of the final 3D prototype to perform MC simulations dedicated to made prevision and to help in the understanding of the results that will we obtain during the prototype performance tests.

## REFERENCES

- [1] Cosmic Vision: Space Science for Europe 2015-2025, ESA Brochure Volume BR-247, pp. 1-111 (2005) (<http://sci.esa.int/science-e/www/object/index.cfm?fobjectid=38542#>).
- [2] Frontera, F., et al., "Focusing of gamma-rays with Laue lenses: first results", Proc. SPIE 7011, 70111R 1-8 (2008).
- [3] Lei, F., Dean, A.J. and Hills, G.L., "Compton Polarimetry in Gamma-Ray Astronomy", Space Science Review 82, 309-388 (1997).
- [4] Gehrels, N., et al., "The Swift Gamma-Ray Burst Mission", The Astrophysical Journal 711(2), 1005-1020 (2004).
- [5] Lebrun, F., et al., "ISGRI : a CdTe array imager for INTEGRAL", Proc. SPIE 2806, 258-268 (1996).
- [6] Meuris, A., et al., "Caliste 64, an Innovative CdTe Hard X-Ray Micro-Camera", IEEE Trans. on Nucl. Sci. 55(2), 778-784 (2008).
- [7] Takeda, S., et al., "A new Si/CdTe semiconductor Compton camera developed for high-angular resolution", Proc. SPIE 6706, 67060S 1-11 (2007).
- [8] Caroli, E., et al., "A focal plane detector design for a wide band Laue-lens telescope", Proc. SPIE 6266, 62662A 1-12 (2006).
- [9] Caroli, E., et al., "A three-dimensional CZT detector as a focal plane prototype for a Laue Lens telescope", Proc. SPIE 7011, 70113G 1-10 (2008).
- [10] Casali, F., et al., "Characterization of small CdTe detectors to be used for linear and matrix arrays", IEEE Trans. on Nucl. Sci. 39(4), 598-604 (1992).
- [11] Van Pamelén, M.A.J., Budtz-Jørgensen, C. and Kuvvetli, I., "Development of CdZnTe X-ray detectors at DSRI", Nucl. Instr. and Meth. in Phys Res. A 439, 625-633 (2000).
- [12] Gostilo, V., et al., "The development of drift-strip detectors based on CdZnTe", IEEE Trans. on Nucl. Sci. 49(5), 2530-2534 (2002).
- [13] Dusi, W., et al., "Spectroscopic behavior of CdTe detectors as a function of the inter-electrode distance", Proc. SPIE 3768, 88-97 (1999).
- [14] Zappettini, A., et al., "Boron oxide encapsulated vertical bridgman grown CdZnTe crystals as X-Ray detector material", IEEE Trans. on Nucl. Sci. 56(4), 1743-1746 (2009).
- [15] Curado da Silva, R.M., et al., "Polarimetric performance of a Laue lens gamma-ray CdZnTe focal plane prototype", Journal of Applied Physics 104, 084903 1-7 (2008).